

# Loss or Gain of Function? Ion Channel Mutation Effects on Neuronal Firing Depend on Cell Type

## 1 **Abstract (250 Words Maximum - Currently 231)**

2 Ion channels determine neuronal excitability and disruption in ion channel properties in mutations  
3 can result in neurological disorders called channelopathies. Often many mutations are associated  
4 with a channelopathy, and determination of the effects of these mutations are generally done at the  
5 level of currents. The impact of such mutations on neuronal firing is vital for selecting personalized  
6 treatment plans for patients, however whether the effect of a given mutation on firing can simply be  
7 inferred from current level effects is unclear. The general impact of the ionic current environment  
8 in different neuronal types on the outcome of ion channel mutations is vital to understanding of  
9 the impacts of ion channel mutations and effective selection of personalized treatments. Using a  
10 diverse collection of neuronal models, the effects of changes in ion current properties on firing is  
11 assessed systematically and for episodic ataxia type 1 associated  $K_v1.1$  mutations. The effects of  
12 ion current property changes or mutations on firing is dependent on the current environment, or cell  
13 type, in which such a change occurs in. Characterization of ion channel mutations as loss or gain of  
14 function is useful at the level of the ionic current, however the effects of channelopathies on firing  
15 is dependent on cell type. To further the efficacy of personalized medicine in channelopathies, the  
16 effects of ion channel mutations must be examined in the context of the appropriate cell types.

## 17 **Significant Statement (120 Words Maximum - Currently 112)**

18 Ion channels determine neuronal excitability and mutations that alter ion channel properties result  
19 in neurological disorders called channelopathies. Although the genetic nature of such mutations  
20 as well as their effects on the ion channel's biophysical properties are routinely assessed exper-  
21 imentally, determination of the role in altering neuronal firing is more difficult. Computational  
22 modelling bridges this gap and demonstrates that the cell type in which a mutation occurs is an  
23 important determinant in the effects of firing. As a result, classification of ion channel mutations  
24 as loss or gain of function is useful to describe the ionic current but care should be taken when  
25 applying this classification on the level of neuronal firing.

## 26 **Introduction (750 Words Maximum - Currently 673)**

27 Neuronal ion channels are vital in determining neuronal excitability, action potential generation and  
28 firing patterns ([Bernard and Shevell, 2008](#); [Carbone and Mori, 2020](#)). In particular, the properties  
29 and combinations of ion channels and their resulting currents determine the firing properties of the  
30 neuron ([Pospischil et al., 2008](#); [Rutecki, 1992](#)). However, ion channel function can be disturbed,  
31 resulting in altered ionic current properties and altered neuronal firing behaviour ([Carbone and](#)  
32 [Mori, 2020](#)). Ion channel mutations are a common cause of such channelopathies and are often  
33 associated with hereditary clinical disorders ([Bernard and Shevell, 2008](#); [Carbone and Mori, 2020](#)).  
34 The effects of these mutations are frequently determined at a biophysical level, however assessment  
35 of the impact of mutations on neuronal firing and excitability is more difficult. Experimentally,  
36 transfection of cell cultures or the generation of mutant mice lines are common approaches. Cell  
37 culture transfection does not replicate the exact interplay of endogenous currents nor does it take  
38 into account the complexity of the nervous system including factors such as expression patterns,

39 intracellular regulation and modulation of ion channels as well as network effects. Transfected  
40 currents are characterized in isolation and the role of these isolated currents in the context of other  
41 currents in a neuron cannot be definitively inferred. The effects of individual currents *in vivo* also  
42 depend on the neuron type they are expressed in and which roles these neurons have in specific  
43 circuits. Complex interactions between different cell types *in vivo* are neglected in transfected cell  
44 culture. Additionally, transfected currents are not present with the neuron-type specific cellular  
45 machinery present *in vivo* and are even transfected in cells of different species. Furthermore, culture  
46 conditions can shape ion channel expression (Ponce et al., 2018).

47 Ion channel transfection of primary neuronal cultures can overcome some of the limitations of cell  
48 culture expression. In transfected neuronal cell cultures firing can more readily be assessed as en-  
49 dogenous currents are present, however the expressed and endogenous versions of the same ion  
50 channel are present in the cell (Scalmani et al., 2006; Smith et al., 2018). To avoid the confound of  
51 both expressed and endogenous current contributing to firing, a drug resistance can be introduced  
52 into the ion channel that is transfected and the drug is used to silence the endogenous version  
53 of this current (Liu et al., 2019). Although addition of TTX-resistance to Na<sub>v</sub> does not alter the  
54 gating properties of these channels (Leffler et al., 2005), the relative expression and conductance  
55 of the transfected ion channel in relation to endogenous currents can be variable and non-specific  
56 blocking of ion channels not affected by the channelopathy may occur. As the firing behaviour  
57 and dynamics of neuronal models can be dramatically altered by altering relative current ampli-  
58 tudes (Barreiro et al., 2012; Golowasch et al., 2002; Kispersky et al., 2012; Pospischil et al., 2008;  
59 Rutecki, 1992), primary neuronal cultures provide a useful general indication as to the effects of  
60 ion channel mutations but do not provide definitive insight into the effects of a channelopathy on  
61 *in vivo* firing.

62 The generation of mice lines is costly and behavioural characterization of new mice lines is required  
63 to assess similarities to patient symptoms. Although the generation of mouse lines is desirable for

a clinical disorder characterized by a specific ion channel mutation, this approach becomes impractical for disorders associated with a collection of distinct mutations in a single ion channel. Because of the lack of adequate experimental approaches, a great need is present for the ability to assess the impacts of ion channel mutations on neuronal firing. A more general understanding of the effects of changes in current properties on neuronal firing may help to understand the impacts of ion channel mutations. Specifically, modelling approaches can be used to assess the impacts of current property changes on firing behaviour, bridging the gap between changes in the biophysical properties induced by mutations and clinical symptoms. Conductance-based neuronal models enable insight into the effects of ion channel mutations with specific effects of the resulting ionic current as well as enabling *in silico* assessment of the relative effects of changes in biophysical properties of ionic currents on neuronal firing . The effects of altered voltage-gated potassium channel K<sub>V</sub>1.1 function is of particular interest in this study as it gives rise to the I<sub>K<sub>V</sub>1.1</sub> current and is associated with episodic ataxia type 1. Furthermore, modelling approaches enable predictions of the effects of specific mutation and drug induced biophysical property changes.

K<sub>V</sub>1.1 channels, encoded by the KCNA1 gene, play a role in repolarizing the action potential, neuronal firing patterns, neurotransmitter release, and saltatory conduction (D'Adamo et al., 1998) and are expressed throughout the CNS (Tsaour et al., 1992; Veh et al., 1995; Wang et al., 1994). Altered K<sub>V</sub>1.1 channel function as a result of KCNA1 mutations in humans is associated with episodic ataxia type 1 (EA1) which is characterized by period attacks of ataxia and persistent myokymia (Parker, 1946; Van Dyke et al., 1975). Onset of EA1 is before 20 years of age (Brunt and van Weerden, 1990; Jen et al., 2007; Rajakulendran et al., 2007; Van Dyke et al., 1975) and is associated with a 10 times higher prevalence of epileptic seizures (Zuberi et al., 1999). EA1 significantly impacts patient quality of life (Graves et al., 2014). K<sub>V</sub>1.1 null mice have spontaneous seizures without ataxia starting in the third postnatal week although impaired balance has been reported (Smart et al., 1998; Zhang et al., 1999) and neuronal hyperexcitability has been demonstrated in

these mice ([Brew et al., 2003](#); [Smart et al., 1998](#)). However, the lack of ataxia in  $K_V1.1$  null mice raises the question if the hyperexcitability seen is representative of the effects of EA1 associated  $K_V1.1$  mutations.

Using a diverse set of conductance-based neuronal models we examine the role of current environment on the impact of alterations in channels properties on firing behavior generally and for EA1 associated  $K_V1.1$  mutations.

## Materials and Methods

All modelling and simulation was done in parallel with custom written Python 3.8 software, run on a Cent-OS 7 server with an Intel(R) Xeon (R) E5-2630 v2 CPU.

### Different Cell Models

A group of neuronal models representing the major classes of cortical and thalamic neurons including regular spiking pyramidal (RS pyramidal), regular spiking inhibitory (RS inhibitory), and fast spiking (FS) cells were used ([Pospischil et al., 2008](#)). To each of these models, a  $K_V1.1$  current ( $I_{K_V1.1}$ ); ([Ranjan et al., 2019](#)) was added. A cerebellar stellate cell model from ([Alexander et al., 2019](#)) is used (Cb stellate). This model was also used with a  $K_V1.1$  current ( $I_{K_V1.1}$ ; ([Ranjan et al., 2019](#))) in addition to the A-type potassium current (Cb stellate + $K_V1.1$ ) or replacing the A-type potassium current (Cb stellate  $\Delta K_V1.1$ ). A subthalamic nucleus neuron model as described by ([Otsuka et al., 2004](#)) are used (STN) and with a  $K_V1.1$  current ( $I_{K_V1.1}$ ; ([Ranjan et al., 2019](#))) in addition to the A-type potassium current (STN + $K_V1.1$ ) or replacing the A-type potassium current (STN  $\Delta K_V1.1$ ). The properties and conductances of each model are detailed in Table 1 and the

gating properties are unaltered from the original Cb stellate and STN models. For comparability to typical electrophysiological data fitting reported and for ease of further gating curve manipulations, a Boltzmann function

$$x_{\infty} = \left( \frac{1 - a}{1 + \exp\left[\frac{V - V_{1/2}}{k}\right]} + a \right)^j \quad (1)$$

with slope  $k$ , voltage for half-maximal activation or inactivation ( $V_{1/2}$ ), exponent  $j$ , and persistent current  $0 \leq a \leq 1$  were fitted for the RS pyramidal, RS inhibitory and FS models (Pospischil et al., 2008). The properties of  $I_{K_{V1.1}}$  were fitted to the mean wild type biophysical parameters of  $K_{V1.1}$  (Lauxmann et al., 2021).

## Firing Frequency Analysis

The membrane responses to 200 equidistant two second long current steps were simulated using the forward-Euler method with a  $\Delta t = 0.01$  ms from steady state. Current steps ranged from 0 to 1 nA for all models except for the RS inhibitory neuron models where a range of 0 to 0.35 nA was used to ensure repetitive firing across the range of input currents. For each current step, action potentials were detected as peaks with at least 50 mV prominence and a minimum interspike interval of 1 ms. The interspike interval was computed and used to determine the instantaneous firing frequencies elicited by the current step. The steady-state firing frequency were defined as the mean firing frequency in 0.5 seconds after the first action potential in the last second of the current step respectively and was used to construct frequency-current (fI) curves.

The smallest current at which steady state firing occurs was identified and the current step interval preceding the occurrence of steady state firing was simulated at higher resolution (100 current steps) to determine the current at which steady state firing began. Firing was simulated with 100 current steps from this current upwards for 1/5 of the overall current range. Over this range a fI

	RS Pyra- midal	RS Inhib- itory	FS	Cb Stellate	Cb Stellate +K <sub>V</sub> 1.1	Cb Stellate $\Delta$ K <sub>V</sub> 1.1	STN	STN +K <sub>V</sub> 1.1	STN $\Delta$ K <sub>V</sub> 1.1
$g_{Na}$	56	10	58	3.4	3.4	3.4	49	49	49
$g_K$	5.4	1.89	3.51	9.0556	8.15	9.0556	57	56.43	57
$g_{K_V1.1}$	0.6	0.21	0.39	—	0.90556	1.50159	—	0.57	0.5
$g_A$	—	—	—	15.0159	15.0159	—	5	5	—
$g_M$	0.075	0.0098	0.075	—	—	—	—	—	—
$g_L$	—	—	—	—	—	—	5	5	5
$g_T$	—	—	—	0.45045	0.45045	0.45045	5	5	5
$g_{Ca,K}$	—	—	—	—	—	—	1	1	1
$g_{Leak}$	0.0205	0.0205	0.038	0.07407	0.07407	0.07407	0.035	0.035	0.035
$\tau_{max,M}$	608	934	502	—	—	—	—	—	—
$C_m$	118.44	119.99	101.71	177.83	177.83	177.83	118.44	118.44	118.44

Table 1: Cell properties and conductances of regular spiking pyramidal neuron (RS Pyramidal), regular spiking inhibitory neuron (RS Inhibitory), fast spiking neuron (FS), cerebellar stellate cell (Cb Stellate), with additional  $I_{K_V1.1}$  (Cb Stellate  $\Delta K_V1.1$  ) and with  $I_{K_V1.1}$  replacement of  $I_A$  (Cb Stellate  $\Delta K_V1.1$  ), and subthalamic nucleus neuron (STN), with additional  $I_{K_V1.1}$  (STN  $\Delta K_V1.1$  ) and with  $I_{K_V1.1}$  replacement of  $I_A$  (STN  $K_V1.1$  ) models. All conductances are given in mS/cm<sup>2</sup>. Capacitances ( $C_m$ ) and  $\tau_{max,M}$  are given in pF and ms respectively.

130 curve was constructed and the integral, or area under the curve (AUC), of the fl curve over this  
131 interval was computed with the composite trapezoidal rule and used as a measure of firing rate  
132 independent from rheobase.

133 To obtain the rheobase, the current step interval preceding the occurrence of action potentials was  
134 explored at higher resolution with 100 current steps spanning the interval. Membrane responses to  
135 these current steps were then analyzed for action potentials and the rheobase was considered the  
136 lowest current step for which an action potential was elicited.

137 All models exhibit tonic firing and any instances of bursting were excluded to simplify the charac-

	Gating	$V_{1/2}$ [mV]	$k$	$j$	$a$
	$I_{Na}$ activation	-34.33054521	-8.21450277	1.42295686	—
RS pyramidal,	$I_{Na}$ inactivation	-34.51951036	4.04059373	1	0.05
RS inhibitory,	$I_{Kd}$ activation	-63.76096946	-13.83488194	7.35347425	—
FS	$I_L$ activation	-39.03684525	-5.57756176	2.25190197	—
	$I_L$ inactivation	-57.37	20.98	1	—
	$I_M$ activation	-45	-9.9998807337	1	—
$I_{Kv1.1}$	$I_{Kv1.1}$ activation	-30.01851852	-7.73333333	1	—
	$I_{Kv1.1}$ Inactivation	-46.85851852	7.67266667	1	0.245

Table 2: For comparability to typical electrophysiological data fitting reported and for ease of further gating curve manipulations, a Boltzmann  $x_\infty = \left( \frac{1-a}{1+\exp[\frac{V-V_{1/2}}{k}]} + a \right)^j$  with slope  $k$ , voltage for half-maximal activation or inactivation ( $V_{1/2}$ ), exponent  $j$ , and persistent current  $0 \leq a \leq 1$  were fitted for the (Pospischil et al., 2008) models where  $\alpha_x$  and  $\beta_x$  are used. Gating parameters for  $I_{Kv1.1}$  are taken from (Ranjan et al., 2019) and fit to mean wild type parameters in (Lauxmann et al., 2021). Model gating not listed are taken directly from source publication.

138 terization of firing.

### 139 Sensitivity Analysis and Comparison of Models

140 Current properties of currents common to all models ( $I_{Na}$ ,  $I_K$ ,  $I_A/I_{Kv1.1}$ , and  $I_{Leak}$ ) were systemati-  
141 cally altered in a one-factor-at-a-time sensitivity analysis for all models. The gating curves for each  
142 current were shifted ( $\Delta V_{1/2}$ ) from -10 to 10 mV in increments of 1 mV. The slope ( $k$ ) of the gating  
143 curves were altered from half to twice the initial slope. Similarly, the maximal current conductance  
144 ( $g$ ) was also scaled from half to twice the initial value. For both slope and conductance alterations,  
145 alterations consisted of 21 steps spaced equally on a  $\log_2$  scale.



## 146 **Model Comparison**

Changes in rheobase ( $\Delta rheobase$ ) are calculated in relation to the original model rheobase. The contrast of each AUC value ( $AUC_i$ ) was computed in comparison to the AUC of the unaltered wild type model ( $AUC_{wt}$ )

$$AUC_{contrast} = \frac{AUC_i - AUC_{wt}}{AUC_{wt}} \quad (2)$$

147 To assess whether the effects of a given alteration on  $AUC_{contrast}$  or  $\Delta rheobase$  are robust across  
148 models, the correlation between  $AUC_{contrast}$  or  $\Delta rheobase$  and the magnitude of current property  
149 alteration was computed for each alteration in each model and compared across alteration types.

150 The Kendall's  $\tau$  coefficient, a non-parametric rank correlation, is used to describe the relationship  
151 between the magnitude of the alteration and AUC or rheobase values. A Kendall  $\tau$  value of -1 or 1  
152 is indicative of monotonically decreasing and increasing relationships respectively.

## 153 **KCNA1/K<sub>V</sub>1.1 Mutations**

154 Known episodic ataxia type 1 associated KCNA1 mutations and their electrophysiological charac-  
155 terization reviewed in (Lauxmann et al., 2021). The mutation-induced changes in  $I_{K_{V1.1}}$  amplitude  
156 and activation slope ( $k$ ) were normalized to wild type measurements and changes in activation  $V_{1/2}$   
157 were used relative to wild type measurements. The effects of a mutation were also applied to  $I_A$   
158 when present as both potassium currents display prominent inactivation. In all cases, the muta-  
159 tion effects were applied to half of the  $K_{V1.1}$  or  $I_A$  under the assumption that the heterozygous  
160 mutation results in 50% of channels carrying the mutation. Frequency-current curves for each mu-  
161 tation in each model were obtained through simulation and used to characterize firing behaviour as  
162 described above. For each model the differences in mutation AUC to wild type AUC were normal-  
163 ized by wild type AUC ( $AUC_{contrast}$ ) and mutation rheobases are compared to wild type rheobase

164 values ( $\Delta rheobase$ ). Pairwise Kendall rank correlations (Kendall  $\tau$ ) are used to compare the the  
165 correlation in the effects of  $K_V1.1$  mutations on AUC and rheobase between models.

## 166 **Code Accessibility**

167 The code/software described in the paper is freely available online at [URL redacted for double-  
168 blind review]. The code is available as Extended Data.

## 169 **Results**

170 To examine the role of cell specific current environments on the impact of altered ion channel  
171 properties on firing behaviour a set of neuronal models is used and properties of channels common  
172 across models are altered systematically one at a time. The effects of a set of episodic ataxia type  
173 1 associated  $K_V1.1$  mutations on firing was then examined across different neuronal models with  
174 different current environments.

## 175 **Firing Characterization**

176 Neuronal firing is a complex phenomenon and classification of firing is needed for comparability  
177 across cell types. Here we focus on the classification of two aspects of firing: rheobase (smallest  
178 injected current at which the cell fires an action potential) and the initial shape of the frequency-  
179 current (fI) curve. The quantification of the initial shape of the fI curve using by computing the area  
180 under the curve (AUC) is a measure of the initial firing at currents above rheobase (Figure 1A).  
181 The characterization of firing with AUC and rheobase enables determination of general increases  
182 or decreases in firing based on current-firing relationships, with the upper left quadrant ( $+\Delta AUC$   
183 and  $-\Delta rheobase$ ) indicate an increase in firing, whereas the bottom right quadrant ( $-\Delta AUC$  and  
184  $+\Delta rheobase$ ) is indicative of decreased firing (Figure 1B). In the lower left and upper right quad-

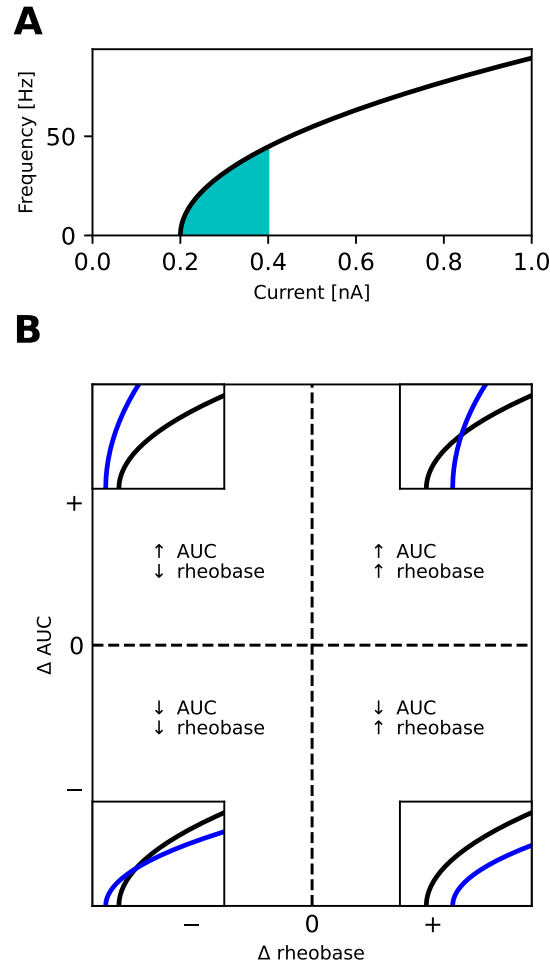


Figure 1: Characterization of firing with AUC and rheobase. (A) The area under the curve (AUC) of the repetitive firing frequency-current (fI) curve. (B) Changes in firing as characterized by  $\Delta$ AUC and  $\Delta$ rheobase occupy 4 quadrants separated by no changes in AUC and rheobase. Representative schematic fI curves in blue with respect to a reference fI curve (black) depict the general changes associated with each quadrant.

185 rants, the effects on firing are more nuance and cannot easily be described as a gain or loss of  
 186 excitability.

187 Considerable diversity is present in the set of neuronal models used as evident in the variability  
 188 seen across neuronal models both in representative spike trains and their fI curves (Figure 2). The

models chosen all fire repetitively and do not exhibit bursting. Some models, such as Cb stellate and RS inhibitory models, display type I firing whereas others such as Cb stellate  $\Delta K_V 1.1$  and STN models have type II firing. Type I firing is characterized by continuous fI curve (i.e. firing rate is continuous) generated through a saddle-node on invariant cycle bifurcation and type II firing is characterized by a discontinuity in the fI curve (i.e. a jump occurs from no firing to firing at a certain frequency) due to a Hopf bifurcation (Ermentrout, 1996; Ermentrout and Chow, 2002). Other models lie on a continuum between these prototypical firing classifications. Most neuronal models exhibit hysteresis with ascending and descending ramps eliciting spikes with different thresholds, however STN +  $K_V 1.1$ , STN  $\Delta K_V 1.1$ , Cb stellate  $\Delta K_V 1.1$  have large hysteresis (Figure 2).

## Sensitivity analysis

A one-factor-at-a-time sensitivity analysis enables the comparison of a given alteration in current parameters across models. Changes in gating  $V_{1/2}$  and slope factor  $k$  as well as the current conductance affect AUC (Figure 3 A, B and C). Heterogeneity in the correlation between gating and conductance changes and AUC occurs across models for most currents. In these cases some of the models display non-monotonic relationships (i.e.  $|\text{Kendall } \tau| \neq 1$ ). However, shifts in A current activation  $V_{1/2}$ , changes in  $K_V 1.1$  activation  $V_{1/2}$  and slope, and changes in A current conductance display consistent monotonic relationships across models.

Alterations in gating  $V_{1/2}$  and slope factor  $k$  as well as the current conductance also play a role in determining rheobase (Figure 4 A, B and C). Shifts in half activation of gating properties are similarly correlated with rheobase across models, however Kendall  $\tau$  values departing from -1 indicate non-monotonic relationships between K current  $V_{1/2}$  and rheobase in some models (Figure 4A). Changes in Na current inactivation,  $K_V 1.1$  current inactivation and A current activation have affect rheobase with positive and negative correlations in different models (Figure 4B). Departures from

213 monotonic relationships occur in some models as a result of K current activation, K<sub>V</sub>1.1 current  
214 inactivation and A current activation in some models. Current conductance magnitude alterations  
215 affect rheobase similarly across models (Figure 4C).

## 216 **K<sub>V</sub>1.1**

217 The changes in AUC and rheobase from wild-type values for reported episodic ataxia type 1 (EA1)  
218 associated K<sub>V</sub>1.1 mutations are heterogenous across models containing K<sub>V</sub>1.1 , but generally show  
219 decreases in rheobase (Figure 5A-I). Pairwise non-parametric Kendall  $\tau$  rank correlations between  
220 the simulated effects of these K<sub>V</sub>1.1 mutations on rheobase are highly correlated across models  
221 (Figure 5J). However, the effects of the K<sub>V</sub>1.1 mutations on AUC are more heterogenous as re-  
222 flected by both weak and strong positive and negative pairwise correlations between models (Fig-  
223 ure 5K).

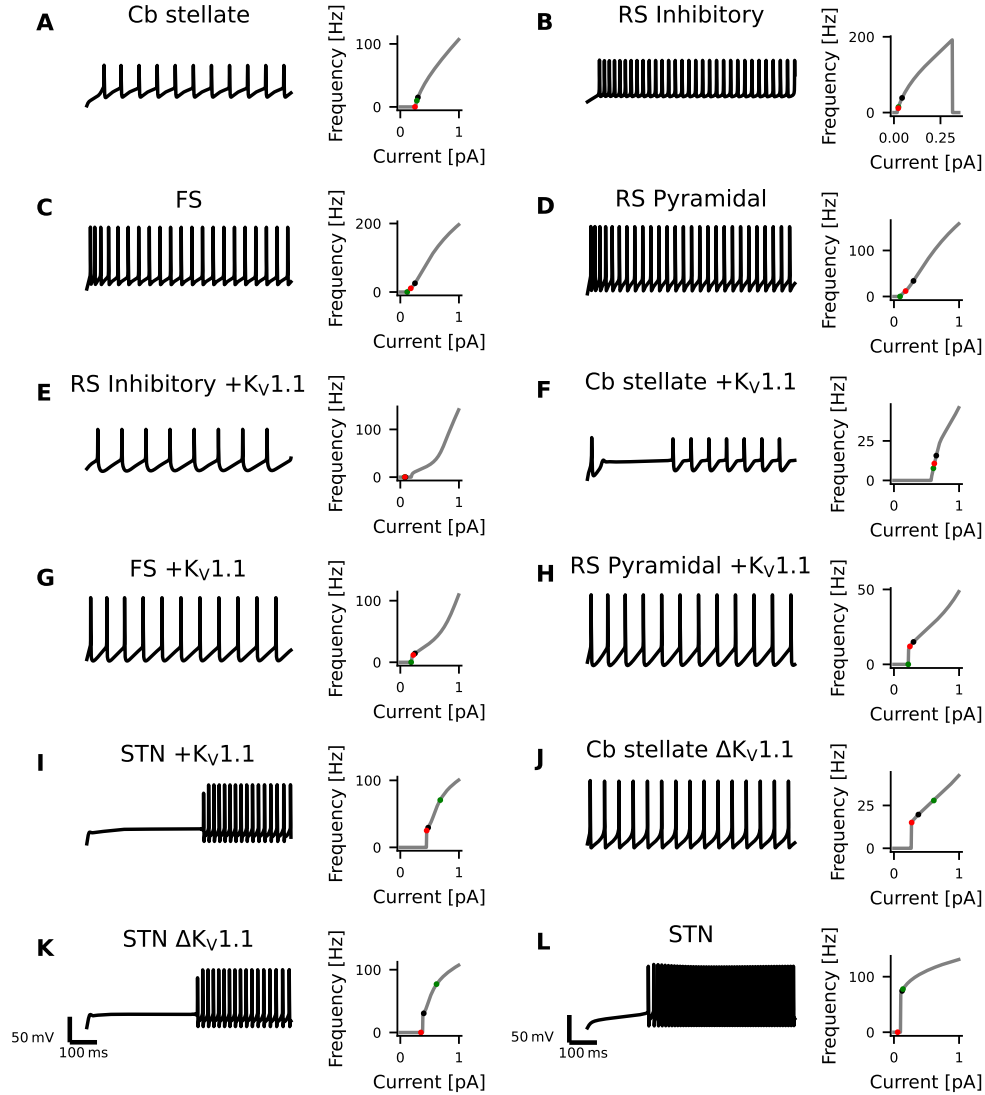


Figure 2: Diversity in Neuronal Model Firing. Spike trains (left), frequency-current (fI) curves (right) for Cb stellate (A), RS inhibitory (B), FS (C), RS pyramidal (D), RS inhibitory + $K_V1.1$  (E), Cb stellate + $K_V1.1$  (F), FS + $K_V1.1$  (G), RS pyramidal + $K_V1.1$  (H), STN + $K_V1.1$  (I), Cb stellate  $\Delta K_V1.1$  (J), STN  $\Delta K_V1.1$  (K), and STN (L) neuron models. Black marker on the fI curves indicate the current step at which the spike train occurs. The green marker indicates the current at which firing begins in response to an ascending current ramp, whereas the red marker indicates the current at which firing ceases in response to a descending current ramp (see Figure 2-1).

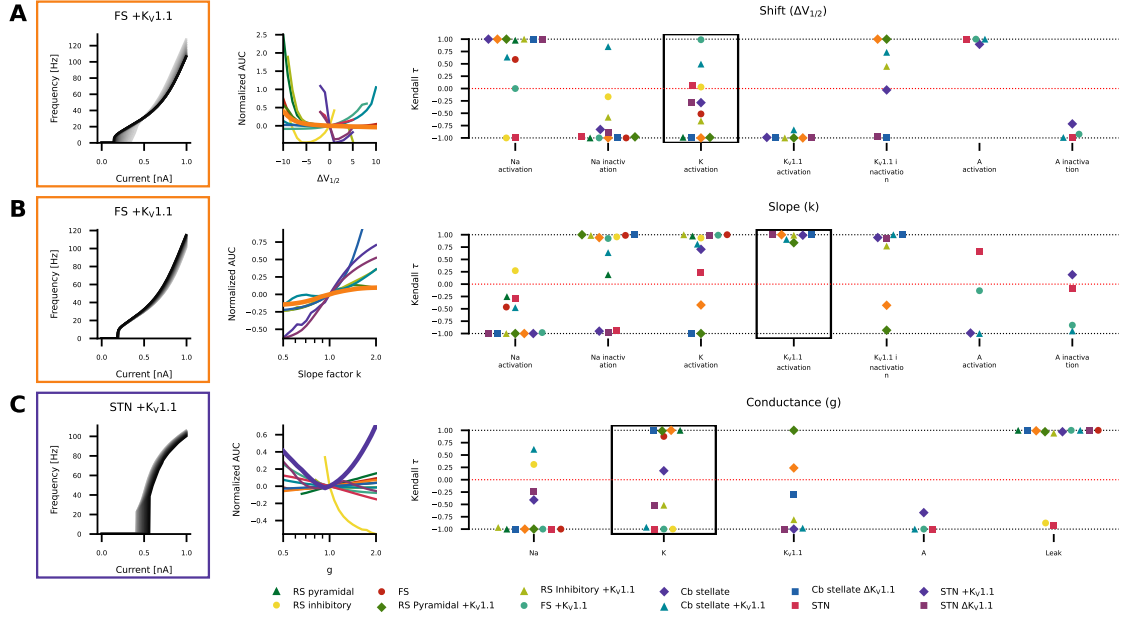


Figure 3: The Kendall rank correlation (Kendall  $\tau$ ) coefficients between shifts in  $V_{1/2}$  and AUC, slope factor  $k$  and AUC as well as current conductances and AUC for each model are shown on the right in (A), (B) and (C) respectively. The relationships between AUC and  $\Delta V_{1/2}$ , slope ( $k$ ) and conductance ( $g$ ) for the Kendall  $\tau$  coefficients highlights by the black box are depicted in the middle panel. The FI curves corresponding to one of the models are shown in the left panels.

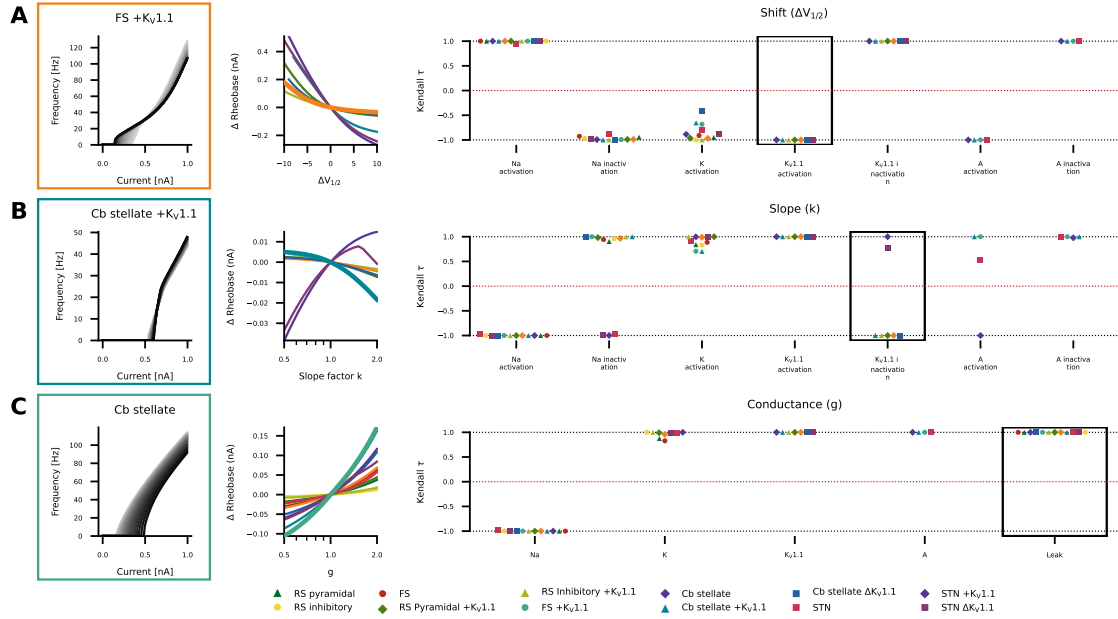


Figure 4: The Kendall rank correlation (Kendall  $\tau$ ) coefficients between shifts in  $V_{1/2}$  and rheobase, slope factor  $k$  and AUC as well as current conductances and rheobase for each model are shown on the right in (A), (B) and (C) respectively. The relationships between rheobase and  $\Delta V_{1/2}$ , slope ( $k$ ) and conductance ( $g$ ) for the Kendall  $\tau$  coefficients highlights by the black box are depicted in the middle panel. The fI curves corresponding to one of the models are shown in the left panels.



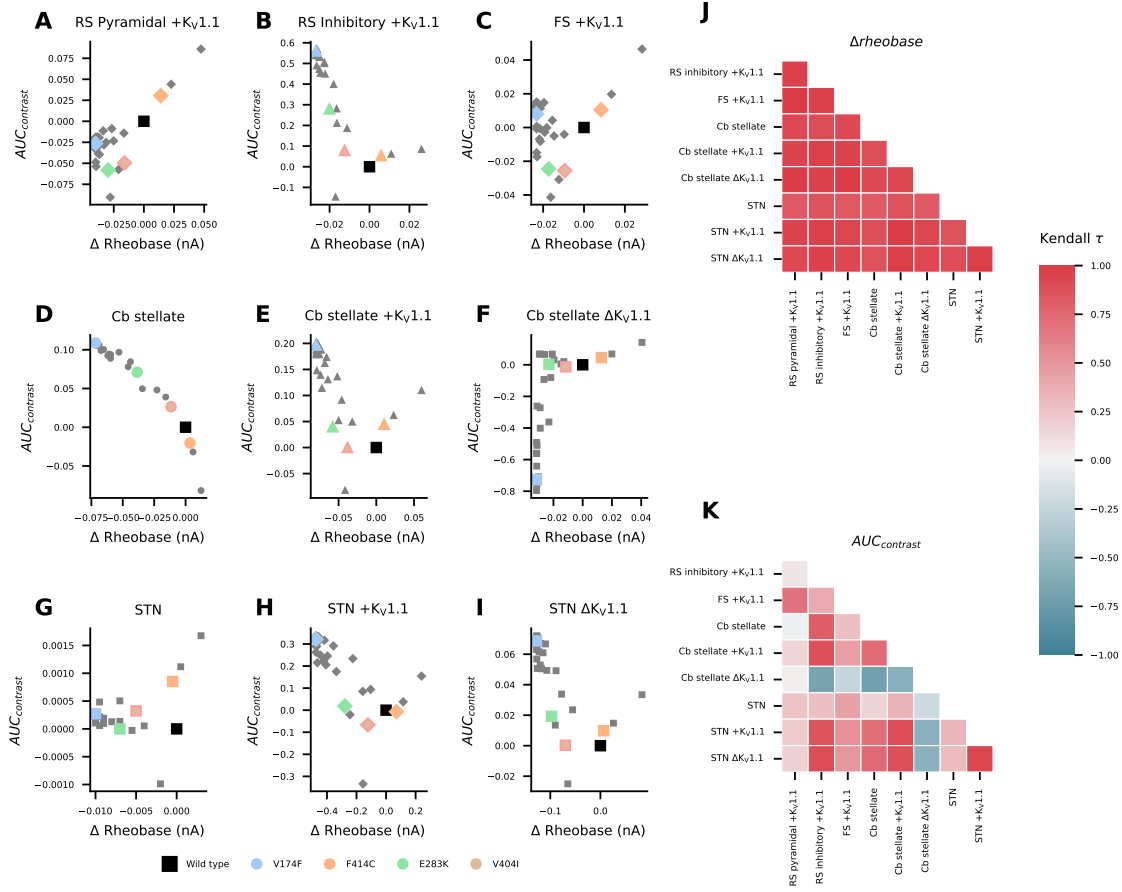


Figure 5: Effects of episodic ataxia type 1 associated  $K_V1.1$  mutations on firing. Effects of  $K_V1.1$  mutations on AUC ( $AUC_{contrast}$ ) and rheobase ( $\Delta$ rheobase) compared to wild type for RS pyramidal +  $K_V1.1$  (A), RS inhibitory +  $K_V1.1$  (B), FS +  $K_V1.1$  (C), Cb stellate (D), Cb stellate +  $K_V1.1$  (E), Cb stellate  $\Delta K_V1.1$  (F), STN (G), STN +  $K_V1.1$  (H) and STN  $\Delta K_V1.1$  (I) models V174F, F414C, E283K, and V404I mutations are highlighted in color for each model. Pair-wise Kendall rank correlation coefficients (Kendall  $\tau$ ) between the effects of  $K_V1.1$  mutations on rheobase and on AUC are shown in J and K respectively.

## Discussion (3000 Words Maximum - Currently 1780)

Using a set of diverse conductance-based neuronal models, the effects of changes to current properties and conductances on firing were determined to be heterogenous for the AUC of the steady state fI curve but more homogenous for rheobase. For a known channelopathy, episodic ataxia type 1 associated  $K_V1.1$  mutations, the effects on rheobase is consistent across cell types, whereas the effect on AUC is cell type dependent.

### Validity of Neuronal Models

The  $K_V1.1$  model from (Ranjan et al., 2019) is based on expression of only  $K_V1.1$  in CHO cells and represents the biophysical properties of  $K_V1.1$  homotetramers and not heteromers. Thus the  $K_V1.1$  model used here neglects the complex reality of these channels *in vivo* including their expression as heteromers and the altered biophysical properties of these heteromers (Coleman et al., 1999; Isacoff et al., 1990; Rettig et al., 1994; Roeper et al., 1998; Ruppersberg et al., 1990; Wang et al., 1999). Furthermore, dynamic modulation of  $K_V1.1$  channels, although physiologically relevant, is neglected here. For example,  $K_V\beta2$  plays a role in  $K_V1$  channel trafficking and cell membrane expression (Campomanes et al., 2002; Manganas et al., 2001; Shi et al., 2016) and  $K_V1.1$  phosphorylation increases cell membrane  $K_V1.1$  (Jonas and Kaczmarek, 1996). It should be noted that the discrete classification of potassium currents into delayed rectifier and A-type is likely not biological, but rather highlights the characteristics of a spectrum of potassium channel inactivation that arises in part due to additional factors such as heteromer composition (Glasscock, 2019; Stühmer et al., 1989), non-pore forming subunits (e.g.  $K_V\beta$  subunits) (Rettig et al., 1994; Xu and Li, 1997), and temperature (Ranjan et al., 2019) modulating channel properties.

Additionally, the single-compartment model does not take into consideration differential effects on neuronal compartments (i.e. axon, soma, dendrites), possible different spatial cellular distribution

of channel expression across and within these neuronal compartments or across CNS regions nor does it consider different channel types (e.g Nav1.1 vs Nav1.8). More realistic models would consist of multiple compartments, take more currents into account and take the spatial distribution of channels into account, however these models are more computationally expensive, require current specific models and knowledge of the distribution of conductances across the cell. Despite these limitations, each of the models can reproduce physiological firing behaviour of the neurons they represent (Alexander et al., 2019; Otsuka et al., 2004; Pospischil et al., 2008) and capture key aspects of the dynamics of these cell types. The firing characterization was performed on adapted firing and as such currents that cause adaptation are neglected in our analysis.

## **Current Environments Determine the Effect of Ion Channel Mutations**

One-factor-at-a-time (OFAT) sensitivity analyses such as the one performed here are predicated on assumptions of model linearity, and cannot account for interactions between factors (Czitrom, 1999; Saltelli and Annoni, 2010). OFAT approaches are local and not global (i.e. always in reference to a baseline point in the parameter space) and therefore cannot be generalized to the global parameter space unless linearity is met (Saltelli and Annoni, 2010). The local space around the wild type neuron is explored with an OFAT sensitivity analysis without taking interactions between parameters into account. Comparisons between the effects of changes in similar parameters across different models can be made at the wild type locale indicative of experimentally observed neuronal behaviour. In this case, the role of deviations in the ionic current properties from their wild type in multiple neuronal models presented here provides a starting point for understanding the general role of these current properties in neurons. However, a more global approach would provide a more holistic understanding of the parameter space and provide insight into interactions between properties.

Characterization of the effects of a parameter on firing with non-parametric Kendall  $\tau$  correlations

271 takes into account the sign and monotonicity of the correlation. In other words Kendall  $\tau$  coeffi-  
272 cients provide information as to whether changing a parameter is positively or negatively correlated  
273 with AUC or rheobase as well as the extent to which this correlation is positive or negative across  
274 the parameter range examined. Therefore, Kendall  $\tau$  coefficients provide general information as to  
275 the sensitivity of different models to a change in a given current property, however more nuanced  
276 difference between the sensitivities of models to current property changes, such as the slope of the  
277 relationship between parameter change and firing are not included in our analysis.

278 Although, to our knowledge, no comprehensive evaluation of how current environment and cell  
279 type affect the outcome of ion channel mutations, comparisons between the effects of such mu-  
280 tations in certain cells have been reported. For instance, mutations in the SCN1A gene encoding  
281  $\text{Na}_v1.1$  result in epileptic phenotypes by selective hypoexcitability of inhibitory but not excitatory  
282 neurons in the cortex resulting in circuit hyperexcitability ([Hedrich et al., 2014](#)). In CA3 of the hip-  
283 pocampus, mutation of  $\text{Na}_v1.6$  similarly results in increased excitability of pyramidal neurons and  
284 decreased excitability of parvalbumin positive interneurons ([Makinson et al., 2016](#)). Additionally,  
285 the L858H mutation in  $\text{Na}_v1.7$ , associated with erythromyalgia, has been shown to cause hypoex-  
286 citability in sympathetic ganglion neurons and hyperexcitability in dorsal root ganglion neurons  
287 ([Rush et al., 2006](#); [Waxman, 2007](#)). The differential effects of L858H  $\text{Na}_v1.7$  on firing is depen-  
288 dent on the presence or absence of another sodium channel  $\text{Na}_v1.8$  ([Rush et al., 2006](#); [Waxman,](#)  
289 [2007](#)). In a modelling study, it was found that altering the sodium conductance in 2 stomatogastric  
290 ganglion neuron models from a population models decreases rheobase in both models, however  
291 the initial slope of the fI curves (proportional to AUC) is increased in one model and decreased  
292 in the other suggesting that the magnitude of other currents in these models (such as  $\text{K}_d$ ) deter-  
293 mines the effect of a change in sodium current ([Kispersky et al., 2012](#)). These findings, in concert  
294 with our findings suggest that the current environment in which a channelopathy occurs is vital in  
295 determining the outcomes of the channelopathy on firing.

Cell type specific differences in current properties are important in the effects of ion channel mutations, however within a cell type heterogeneity in channel expression levels exists and it is often desirable to generate a population of neuronal models and to screen them for plausibility to biological data in order to capture neuronal population diversity (Marder and Taylor, 2011). The models we used here are originally generated by characterization of current gating properties and by fitting of maximal conductances to experimental data (Alexander et al., 2019; Otsuka et al., 2004; Pospischil et al., 2008; Ranjan et al., 2019). This practice of fixing maximal conductances based on experimental data is limiting as it does not reproduce the variability in channel expression and neuronal firing behaviour of a heterogeneous neuron population (Verma et al., 2020). For example, a model derived from the mean conductances in a sub-population of stomatogastric ganglion "one-spike bursting" neurons fires 3 spikes instead of 1 per burst due to an L shaped distribution of sodium and potassium conductances (Golowasch et al., 2002). Multiple sets of current conductances can give rise to the same patterns of activity also termed degeneracy and differences in neuronal dynamics may only be evident with perturbations (Goaillard and Marder, 2021; Marder and Taylor, 2011). Variability in ion channel expression often correlates with the expression of other ion channels (Goaillard and Marder, 2021) and neurons whose behaviour is similar may possess correlated variability across different ion channels resulting in stability in neuronal phenotype (Lamb and Calabrese, 2013; Soofi et al., 2012; Taylor et al., 2009). The variability of ion currents and degeneracy of neurons may account, at least in part, for the observation that the effect of toxins within a neuronal type is frequently not constant (Khaliq and Raman, 2006; Puopolo et al., 2007; Ransdell et al., 2013).

### Effects of KCNA1 Mutations

Moderate changes in delayed rectifier potassium currents change the bifurcation structure of Hodgkin Huxley model, with changes analogous to those seen with  $K_V1.1$  mutations resulting in

320 increased excitability due to reduced thresholds for repetitive firing (Hafez and Gottschalk, 2020).  
 321 Although the Hodgkin Huxley delayed rectifier lacks inactivation, the increases in excitability seen  
 322 are in line with both score-based and simulation-based predictions of the outcomes of *KCNA1*  
 323 mutations. LOF *KCNA1* mutations generally increase neuronal excitability, however the different  
 324 effects of *KCNA1* mutations across models on AUC are indicative that a certain cell type spe-  
 325 cific complexity exists. Increased excitability seen experimentally with  $K_V1.1$  null mice (Smart  
 326 et al., 1998; Zhou et al., 1998), with pharmacological  $K_V1.1$  block (Chi and Nicol, 2007; Morales-  
 327 Villagrán et al., 1996), by (Hafez and Gottschalk, 2020) and with simulation-based predictions of  
 328 *KCNA1* mutations. Contrary to these results, (Zhao et al., 2020) predicted *in silico* that the depolar-  
 329 izing shifts seen as a result of *KCNA1* mutations broaden action potentials and interfere negatively  
 330 with high frequency action potential firing, however comparability of firing rates is lacking in this  
 331 study. Different current properties, such as the difference in  $I_A$  and  $I_{K_V1.1}$  in the Cb stellate and  
 332 STN model families alter the impact of *KCNA1* mutations on firing highlighting that knowledge of  
 333 the biophysical properties of a current and its neuronal expression is vital for holistic understanding  
 334 of the effects of a given ion channel mutation both at a single cell and network level.

### 335 **Loss or Gain of Function Characterizations Do Not Fully Capture Ion Channel Mu-** 336 **tation Effects on Firing**

337 The effects of changes in current properties depend in part on the neuronal model in which they  
 338 occur and can be seen in the variance of correlations (especially in AUC) across models for a given  
 339 current property change. Therefore, relative conductances and gating properties of currents in the  
 340 current environment in which an alteration in current properties occurs plays an important role in  
 341 determining the outcome on firing. The use of loss of function (LOF) and gain of function (GOF)  
 342 is useful at the level of ion channels and whether a mutation results in more or less ionic current,  
 343 however the extension of this thinking onto whether mutations induce LOF or GOF at the level of

344 neuronal firing based on the ionic current LOF/GOF is problematic due to the dependency of neu-  
345 ronal firing changes on the current environment. Thus the direct leap from current level LOF/GOF  
346 characterizations to effects on firing without experimental or modelling-based evidence, although  
347 tempting, should be refrained from and viewed with caution when reported. This is especially  
348 relevant in the recent development of personalized medicine for channelopathies, where a patients  
349 specific channelopathy is identified and used to tailor treatments (Ackerman et al., 2013; Gne-  
350 chi et al., 2021; Helbig and Ellis, 2020; Weber et al., 2017). However, the effects of specific ion  
351 channel mutations are often characterized in expression systems and classified as LOF or GOF to  
352 aid in treatment decisions (Brunklaus et al., 2022; Johannesen et al., 2021; Musto et al., 2020).  
353 Interestingly, both LOF and GOF Nav1.1 mutations can benefit from treatment with sodium chan-  
354 nel blockers (Johannesen et al., 2021), suggesting that the relationship between effects at the level  
355 of ion channels and effects at the level of firing and therapeutics is not linear or evident without  
356 further contextual information. Therefore, this approach must be used with caution and the cell  
357 type which expressed the mutant ion channel must be taken into account. Experimental assessment  
358 of the effects of a patients specific ion channel mutation *in vivo* is not feasible at a large scale due  
359 to time and cost constraints, modelling of the effects of patient specific channelopathies is a de-  
360 sirable approach. Accordingly, for accurate modelling and predictions of the effects of mutations  
361 on neuronal firing, information as to the type of neurons containing the affected channel, and the  
362 properties of the affected and all currents in the affected neuronal type is needed. When modelling  
363 approaches are sought out to overcome the limitations of experimental approaches, care must be  
364 taken to account for model dependency and the generation of relevant cell-type or cell specific  
365 populations of models should be standard in assessing the effects of mutations in specific neurons.

## References

- Ackerman, M. J., Marcou, C. A. and Tester, D. J. (2013), 'Personalized Medicine: Genetic Diagnosis for Inherited Cardiomyopathies/Channelopathies', *Revista Española de Cardiología (English Edition)* **66**(4), 298–307.  
**URL:** <https://www.sciencedirect.com/science/article/pii/S1885585713000376>
- Alexander, R. P. D., Mitry, J., Sareen, V., Khadra, A. and Bowie, D. (2019), 'Cerebellar Stellate Cell Excitability Is Coordinated by Shifts in the Gating Behavior of Voltage-Gated Na<sup>+</sup> and A-Type K<sup>+</sup> Channels', *eNeuro* **6**(3).  
**URL:** <https://www.eneuro.org/content/6/3/ENEURO.0126-19.2019>
- Barreiro, A. K., Thilo, E. L. and Shea-Brown, E. (2012), 'A-current and type I/type II transition determine collective spiking from common input', *Journal of Neurophysiology* **108**(6), 1631–1645.  
**URL:** <https://www.ncbi.nlm.nih.gov/pmc/articles/PMC3544951/>
- Bernard, G. and Shevell, M. I. (2008), 'Channelopathies: A Review', *Pediatric Neurology* **38**(2), 73–85.  
**URL:** <https://www.sciencedirect.com/science/article/pii/S0887899407004584>
- Brew, H. M., Hallows, J. L. and Tempel, B. L. (2003), 'Hyperexcitability and reduced low threshold potassium currents in auditory neurons of mice lacking the channel subunit Kv1.1', *The Journal of Physiology* **548**(1), 1–20.  
**URL:** <https://physoc.onlinelibrary.wiley.com/doi/abs/10.1111/j..2003.t01-1-00001.x>
- Brunklaus, A., Feng, T., Brünger, T., Perez-Palma, E., Heyne, H., Matthews, E., Semsarian, C., Symonds, J. D., Zuberi, S. M., Lal, D. and Schorge, S. (2022), 'Gene variant effects across sodium channelopathies predict function and guide precision therapy', *Brain* p. awac006.  
**URL:** <https://doi.org/10.1093/brain/awac006>
- Brunt, E. R. P. and van Weerden, T. W. (1990), 'Familial Paroxysmal Kinesigenic Ataxia and Continuous Myokymia', *Brain* **113**(5), 1361–1382.  
**URL:** <https://doi.org/10.1093/brain/113.5.1361>
- Campomanes, C. R., Carroll, K. I., Manganas, L. N., Hershberger, M. E., Gong, B., Antonucci, D. E., Rhodes, K. J. and Trimmer, J. S. (2002), 'Kv $\beta$  Subunit Oxidoreductase Activity and Kv1 Potassium Channel Trafficking', *Journal of Biological Chemistry* **277**(10), 8298–8305.  
**URL:** <https://www.sciencedirect.com/science/article/pii/S0021925819364324>
- Carbone, E. and Mori, Y. (2020), 'Ion channelopathies to bridge molecular lesions, channel function, and clinical therapies', *Pflügers Archiv - European Journal of Physiology* **472**(7), 733–738.  
**URL:** <https://doi.org/10.1007/s00424-020-02424-y>



- 400 Chi, X. X. and Nicol, G. D. (2007), ‘Manipulation of the Potassium Channel Kv1.1 and Its Effect  
401 on Neuronal Excitability in Rat Sensory Neurons’, *Journal of Neurophysiology* **98**(5), 2683–  
402 2692.  
403 **URL:** <https://journals.physiology.org/doi/full/10.1152/jn.00437.2007>
- 404 Coleman, S. K., Newcombe, J., Pryke, J. and Dolly, J. O. (1999), ‘Subunit Composition of Kv1  
405 Channels in Human CNS’, *Journal of Neurochemistry* **73**(2), 849–858.  
406 **URL:** <https://onlinelibrary.wiley.com/doi/abs/10.1046/j.1471-4159.1999.0730849.x>
- 407 Czitrom, V. (1999), ‘One-Factor-at-a-Time versus Designed Experiments’, *The American Statisti-*  
408 *cian* **53**(2), 126–131.  
409 **URL:** <https://www.jstor.org/stable/2685731>
- 410 D’Adamo, M. C., Liu, Z., Adelman, J. P., Maylie, J. and Pessia, M. (1998), ‘Episodic ataxia type-1  
411 mutations in the hKv1.1 cytoplasmic pore region alter the gating properties of the channel’, *The*  
412 *EMBO Journal* **17**(5), 1200–1207.  
413 **URL:** <https://www.embopress.org/doi/full/10.1093/emboj/17.5.1200>
- 414 Ermentrout, B. (1996), ‘Type I Membranes, Phase Resetting Curves, and Synchrony’,  
415 *Neural Computation* **8**(5), 979–1001. [\\_eprint: https://direct.mit.edu/neco/article-](https://direct.mit.edu/neco/article-pdf/8/5/979/813352/neco.1996.8.5.979.pdf)  
416 [pdf/8/5/979/813352/neco.1996.8.5.979.pdf](https://direct.mit.edu/neco/article-pdf/8/5/979/813352/neco.1996.8.5.979.pdf).  
417 **URL:** <https://doi.org/10.1162/neco.1996.8.5.979>
- 418 Ermentrout, G. and Chow, C. C. (2002), ‘Modeling neural oscillations’, *Physiology & Behavior*  
419 **77**(4), 629–633.  
420 **URL:** <https://www.sciencedirect.com/science/article/pii/S0031938402008983>
- 421 Glasscock, E. (2019), ‘Kv1.1 channel subunits in the control of neurocardiac function’, *Channels*  
422 **13**(1), 299–307.  
423 **URL:** <https://doi.org/10.1080/19336950.2019.1635864>
- 424 Gneecchi, M., Sala, L. and Schwartz, P. J. (2021), ‘Precision Medicine and cardiac channelopathies:  
425 when dreams meet reality’, *European Heart Journal* **42**(17), 1661–1675.  
426 **URL:** <https://doi.org/10.1093/eurheartj/ehab007>
- 427 Goaillard, J.-M. and Marder, E. (2021), ‘Ion Channel Degeneracy, Variability, and Covariation in  
428 Neuron and Circuit Resilience’, *Annual Review of Neuroscience* .  
429 **URL:** <https://www.annualreviews.org/doi/10.1146/annurev-neuro-092920-121538>
- 430 Golowasch, J., Goldman, M. S., Abbott, L. F. and Marder, E. (2002), ‘Failure of Averaging in the  
431 Construction of a Conductance-Based Neuron Model’, *Journal of Neurophysiology* **87**(2), 1129–  
432 1131.  
433 **URL:** <https://journals.physiology.org/doi/full/10.1152/jn.00412.2001>
- 434 Graves, T. D., Cha, Y.-H., Hahn, A. F., Barohn, R., Salajegheh, M. K., Griggs, R. C., Bundy,  
435 B. N., Jen, J. C., Baloh, R. W., Hanna, M. G. and on behalf of the CINCH Investigators (2014),

- 436 ‘Episodic ataxia type 1: clinical characterization, quality of life and genotype–phenotype corre-  
437 lation’, *Brain* **137**(4), 1009–1018.  
438 **URL:** <https://doi.org/10.1093/brain/awu012>
- 439 Hafez, O. A. and Gottschalk, A. (2020), ‘Altered neuronal excitability in a Hodgkin-Huxley model  
440 incorporating channelopathies of the delayed rectifier potassium channel’, *Journal of Computa-  
441 tional Neuroscience* **48**(4), 377–386.  
442 **URL:** <https://doi.org/10.1007/s10827-020-00766-1>
- 443 Hedrich, U. B., Liautard, C., Kirschenbaum, D., Pofahl, M., Lavigne, J., Liu, Y., Theiss, S., Slotta,  
444 J., Escayg, A., Dihné, M., Beck, H., Mantegazza, M. and Lerche, H. (2014), ‘Impaired action po-  
445 tential initiation in gabaergic interneurons causes hyperexcitable networks in an epileptic mouse  
446 model carrying a human nav1.1 mutation’, *Journal of Neuroscience* **34**(45), 14874–14889.  
447 **URL:** <https://www.jneurosci.org/content/34/45/14874>
- 448 Helbig, I. and Ellis, C. A. (2020), ‘Personalized medicine in genetic epilepsies – possibilities,  
449 challenges, and new frontiers’, *Neuropharmacology* **172**, 107970.  
450 **URL:** <https://www.sciencedirect.com/science/article/pii/S0028390820300368>
- 451 Isacoff, E. Y., Jan, Y. N. and Jan, L. Y. (1990), ‘Evidence for the formation of heteromultimeric  
452 potassium channels in *Xenopus* oocytes’, *Nature* **345**(6275), 530–534.  
453 **URL:** <https://www.nature.com/articles/345530a0>
- 454 Jen, J., Graves, T., Hess, E., Hanna, M., Griggs, R., Baloh, R. and the CINCH investigators (2007),  
455 ‘Primary episodic ataxias: diagnosis, pathogenesis and treatment’, *Brain* **130**(10), 2484–2493.  
456 **URL:** <https://doi.org/10.1093/brain/awm126>
- 457 Johannesen, K. M., Liu, Y., Gjerulfsen, C. E., Koko, M., Sonnenberg, L., Schubert, J., Fenger,  
458 C. D., Eltokhi, A., Rannap, M., Koch, N. A., Lauxmann, S., Krüger, J., Kegele, J., Canafoglia,  
459 L., Franceschetti, S., Mayer, T., Rebstock, J., Zacher, P., Ruf, S., Alber, M., Sterbova, K., Las-  
460 suthová, P., Vlckova, M., Lemke, J. R., Krey, I., Heine, C., Wiczorek, D., Kroell-Seger, J.,  
461 Lund, C., Klein, K. M., Au, P. B., Rho, J. M., Ho, A. W., Masnada, S., Veggiotti, P., Giordano,  
462 L., Accorsi, P., Hoei-Hansen, C. E., Striano, P., Zara, F., Verhelst, H., S. Verhoeven, J., Zwaag, B.  
463 v. d., Harder, A. V. E., Brilstra, E., Pendziwiat, M., Lebon, S., Vaccarezza, M., Le, N. M., Chris-  
464 tensen, J., Schmidt-Petersen, M. U., Grønberg, S., Scherer, S. W., Howe, J., Fazeli, W., Howell,  
465 K. B., Leventer, R., Stutterd, C., Walsh, S., Gerard, M., Gerard, B., Matricardi, S., Bonardi,  
466 C. M., Sartori, S., Berger, A., Hoffman-Zacharska, D., Mastrangelo, M., Darra, F., Vølle, A.,  
467 Motazacker, M. M., Lakeman, P., Nizon, M., Betzler, C., Altuzarra, C., Caume, R., Roubertie,  
468 A., Gélisse, P., Marini, C., Guerrini, R., Bilan, F., Tibussek, D., Koch-Hogrebe, M., Perry, M. S.,  
469 Ichikawa, S., Dadali, E., Sharkov, A., Mishina, I., Abramov, M., Kanivets, I., Korostelev, S., Kut-  
470 sev, S., Wain, K. E., Eisenhauer, N., Wagner, M., Savatt, J. M., Müller-Schlüter, K., Bassan, H.,  
471 Borovikov, A., Nassogne, M.-C., Destrée, A., Schoonjans, A.-S., Meuwissen, M., Buzatu, M.,  
472 Jansen, A., Scalais, E., Srivastava, S., Tan, W.-H., Olson, H. E., Loddenkemper, T., Poduri, A.,  
473 Helbig, K. L., Helbig, I., Fitzgerald, M. P., Goldberg, E. M., Roser, T., Borggraefe, I., Brünger,

474 T., May, P., Lal, D., Lederer, D., Rubboli, G., Lesca, G., Hedrich, U. B., Benda, J., Gardella,  
 475 E., Lerche, H. and Møller, R. S. (2021), ‘Genotype-phenotype correlations in SCN8A-related  
 476 disorders reveal prognostic and therapeutic implications’, *medRxiv* p. 2021.03.22.21253711.  
 477 **URL:** <https://www.medrxiv.org/content/10.1101/2021.03.22.21253711v1>

478 Jonas, E. A. and Kaczmarek, L. K. (1996), ‘Regulation of potassium channels by protein kinases’,  
 479 *Current Opinion in Neurobiology* **6**(3), 318–323.  
 480 **URL:** <https://www.sciencedirect.com/science/article/pii/S0959438896801140>

481 Khaliq, Z. M. and Raman, I. M. (2006), ‘Relative Contributions of Axonal and Somatic Na Chan-  
 482 nels to Action Potential Initiation in Cerebellar Purkinje Neurons’, *Journal of Neuroscience*  
 483 **26**(7), 1935–1944.

484 Kispersky, T. J., Caplan, J. S. and Marder, E. (2012), ‘Increase in Sodium Conductance Decreases  
 485 Firing Rate and Gain in Model Neurons’, *Journal of Neuroscience* **32**(32), 10995–11004.  
 486 **URL:** <https://www.jneurosci.org/content/32/32/10995>

487 Lamb, D. G. and Calabrese, R. L. (2013), ‘Correlated Conductance Parameters in Leech Heart  
 488 Motor Neurons Contribute to Motor Pattern Formation’, *PLOS ONE* **8**(11), e79267.  
 489 **URL:** <https://journals.plos.org/plosone/article?id=10.1371/journal.pone.0079267>

490 Lauxmann, S., Sonnenberg, L., Koch, N. A., Boßelmann, C. M., Winter, N., Schwarz, N., Wuttke,  
 491 T. V., Hedrich, U. B. S., Liu, Y., Lerche, H., Benda, J. and Kegele, J. (2021), ‘Therapeutic po-  
 492 tential of sodium channel blockers as targeted therapy approach in KCNA1-associated episodic  
 493 ataxia (EA1) and a comprehensive review of the literature’, *Frontiers in Neurology* **In Press**.  
 494 **URL:** <https://www.frontiersin.org/articles/10.3389/fneur.2021.703970/abstract>

495 Leffler, A., Herzog, R. I., Dib-Hajj, S. D., Waxman, S. G. and Cummins, T. R. (2005), ‘Pharma-  
 496 cological properties of neuronal TTX-resistant sodium channels and the role of a critical serine  
 497 pore residue’, *Pflügers Archiv* **451**(3), 454–463.  
 498 **URL:** <https://doi.org/10.1007/s00424-005-1463-x>

499 Liu, Y., Schubert, J., Sonnenberg, L., Helbig, K. L., Hoei-Hansen, C. E., Koko, M., Rannap, M.,  
 500 Lauxmann, S., Huq, M., Schneider, M. C., Johannesen, K. M., Kurlmann, G., Gardella, E.,  
 501 Becker, F., Weber, Y. G., Benda, J., Møller, R. S. and Lerche, H. (2019), ‘Neuronal mechanisms  
 502 of mutations in SCN8A causing epilepsy or intellectual disability’, *Brain* **142**(2), 376–390.  
 503 **URL:** <https://doi.org/10.1093/brain/awy326>

504 Makinson, C. D., Dutt, K., Lin, F., Papale, L. A., Shankar, A., Barela, A. J., Liu, R., Goldin, A. L.  
 505 and Escayg, A. (2016), ‘An Scn1a epilepsy mutation in Scn8a alters seizure susceptibility and  
 506 behavior’, *Experimental Neurology* **275**, 46–58.  
 507 **URL:** <https://www.sciencedirect.com/science/article/pii/S001448861530090X>

508 Manganas, L. N., Wang, Q., Scannevin, R. H., Antonucci, D. E., Rhodes, K. J. and Trimmer, J. S.  
 509 (2001), ‘Identification of a trafficking determinant localized to the Kv1 potassium channel pore’,

- 510 *Proceedings of the National Academy of Sciences* **98**(24), 14055–14059.  
 511 **URL:** <https://www.pnas.org/content/98/24/14055>
- 512 Marder, E. and Taylor, A. L. (2011), ‘Multiple models to capture the variability in biological neu-  
 513 rons and networks’, *Nature Neuroscience* **14**(2), 133–138.  
 514 **URL:** <https://www.nature.com/articles/nn.2735>
- 515 Morales-Villagrán, A., Ureña-Guerrero, M. E. and Tapia, R. (1996), ‘Protection by NMDA re-  
 516 ceptor antagonists against seizures induced by intracerebral administration of 4-aminopyridine’,  
 517 *European Journal of Pharmacology* **305**(1), 87–93.  
 518 **URL:** <https://www.sciencedirect.com/science/article/pii/S0014299996001574>
- 519 Musto, E., Gardella, E. and Møller, R. S. (2020), ‘Recent advances in treatment of epilepsy-related  
 520 sodium channelopathies’, *European Journal of Paediatric Neurology* **24**, 123–128.  
 521 **URL:** <https://www.sciencedirect.com/science/article/pii/S1090379819304295>
- 522 Otsuka, T., Abe, T., Tsukagawa, T. and Song, W.-J. (2004), ‘Conductance-Based Model of the  
 523 Voltage-Dependent Generation of a Plateau Potential in Subthalamic Neurons’, *Journal of Neu-  
 524 rophysiology* **92**(1), 255–264.  
 525 **URL:** <https://journals.physiology.org/doi/full/10.1152/jn.00508.2003>
- 526 Parker, H. L. (1946), ‘Periodic ataxia’, *Collected Papers of the Mayo Clinic and the Mayo Foun-  
 527 dation. Mayo Clinic* **38**, 642–645.
- 528 Ponce, A., Castillo, A., Hinojosa, L., Martinez-Rendon, J. and Cereijido, M. (2018), ‘The expres-  
 529 sion of endogenous voltage-gated potassium channels in HEK293 cells is affected by culture  
 530 conditions’, *Physiological Reports* **6**(8), e13663.  
 531 **URL:** <https://www.ncbi.nlm.nih.gov/pmc/articles/PMC5903699/>
- 532 Pospischil, M., Toledo-Rodriguez, M., Monier, C., Piwkowska, Z., Bal, T., Frégnac, Y., Markram,  
 533 H. and Destexhe, A. (2008), ‘Minimal Hodgkin–Huxley type models for different classes of  
 534 cortical and thalamic neurons’, *Biological Cybernetics* **99**(4), 427–441.  
 535 **URL:** <https://doi.org/10.1007/s00422-008-0263-8>
- 536 Puopolo, M., Raviola, E. and Bean, B. P. (2007), ‘Roles of Subthreshold Calcium Current and  
 537 Sodium Current in Spontaneous Firing of Mouse Midbrain Dopamine Neurons’, *Journal of Neu-  
 538 roscience* **27**(3), 645–656.
- 539 Rajakulendran, S., Schorge, S., Kullmann, D. M. and Hanna, M. G. (2007), ‘Episodic ataxia type  
 540 1: A neuronal potassium channelopathy’, *Neurotherapeutics* **4**(2), 258–266.  
 541 **URL:** <https://doi.org/10.1016/j.nurt.2007.01.010>
- 542 Ranjan, R., Logette, E., Marani, M., Herzog, M., Tâche, V., Scantamburlo, E., Buchillier, V. and  
 543 Markram, H. (2019), ‘A Kinetic Map of the Homomeric Voltage-Gated Potassium Channel (Kv)  
 544 Family’, *Frontiers in Cellular Neuroscience* **13**.  
 545 **URL:** <https://www.frontiersin.org/articles/10.3389/fncel.2019.00358/full>

- 546 Ransdell, J. L., Nair, S. S. and Schulz, D. J. (2013), 'Neurons within the Same Network Inde-  
547 pendently Achieve Conserved Output by Differentially Balancing Variable Conductance Magni-  
548 tudes', *Journal of Neuroscience* **33**(24), 9950–9956.
- 549 Rettig, J., Heinemann, S. H., Wunder, F., Lorra, C., Parcej, D. N., Oliver Dolly, J. and Pongs, O.  
550 (1994), 'Inactivation properties of voltage-gated K<sup>+</sup> channels altered by presence of  $\beta$ -subunit',  
551 *Nature* **369**(6478), 289–294.  
552 **URL:** <https://www.nature.com/articles/369289a0>
- 553 Roeper, J., Sewing, S., Zhang, Y., Sommer, T., Wanner, S. G. and Pongs, O. (1998), 'NIP domain  
554 prevents N-type inactivation in voltage-gated potassium channels', *Nature* **391**(6665), 390–393.  
555 **URL:** <https://www.nature.com/articles/34916>
- 556 Ruppersberg, J. P., Schröter, K. H., Sakmann, B., Stocker, M., Sewing, S. and Pongs, O.  
557 (1990), 'Heteromultimeric channels formed by rat brain potassium-channel proteins', *Nature*  
558 **345**(6275), 535–537.  
559 **URL:** <https://www.nature.com/articles/345535a0>
- 560 Rush, A. M., Dib-Hajj, S. D., Liu, S., Cummins, T. R., Black, J. A. and Waxman, S. G. (2006),  
561 'A single sodium channel mutation produces hyper- or hypoexcitability in different types of  
562 neurons', *Proceedings of the National Academy of Sciences* **103**(21), 8245–8250.  
563 **URL:** <https://www.pnas.org/doi/10.1073/pnas.0602813103>
- 564 Rutecki, P. A. (1992), 'Neuronal excitability: voltage-dependent currents and synaptic transmis-  
565 sion', *Journal of Clinical Neurophysiology: Official Publication of the American Electroen-*  
566 *cephalographic Society* **9**(2), 195–211.
- 567 Saltelli, A. and Annoni, P. (2010), 'How to avoid a perfunctory sensitivity analysis', *Environmental*  
568 *Modelling & Software* **25**(12), 1508–1517.  
569 **URL:** <https://www.sciencedirect.com/science/article/pii/S1364815210001180>
- 570 Scalmani, P., Rusconi, R., Armatura, E., Zara, F., Avanzini, G., Franceschetti, S. and Mantegazza,  
571 M. (2006), 'Effects in Neocortical Neurons of Mutations of the Nav1.2 Na<sup>+</sup> Channel causing Be-  
572 nign Familial Neonatal-Infantile Seizures', *The Journal of Neuroscience* **26**(40), 10100–10109.  
573 **URL:** <https://www.ncbi.nlm.nih.gov/pmc/articles/PMC6674637/>
- 574 Shi, X.-Y., Tomonoh, Y., Wang, W.-Z., Ishii, A., Higurashi, N., Kurahashi, H., Kaneko, S., Hirose,  
575 S. and Epilepsy Genetic Study Group, Japan (2016), 'Efficacy of antiepileptic drugs for the  
576 treatment of Dravet syndrome with different genotypes', *Brain & Development* **38**(1), 40–46.
- 577 Smart, S. L., Lopantsev, V., Zhang, C. L., Robbins, C. A., Wang, H., Chiu, S. Y., Schwartzkroin,  
578 P. A., Messing, A. and Tempel, B. L. (1998), 'Deletion of the KV1.1 Potassium Channel Causes  
579 Epilepsy in Mice', *Neuron* **20**(4), 809–819.  
580 **URL:** <https://www.sciencedirect.com/science/article/pii/S0896627300810181>

- Smith, R. S., Kenny, C. J., Ganesh, V., Jang, A., Borges-Monroy, R., Partlow, J. N., Hill, R. S., Shin, T., Chen, A. Y., Doan, R. N., Anttonen, A.-K., Ignatius, J., Medne, L., Bönemann, C. G., Hecht, J. L., Salonen, O., Barkovich, A. J., Poduri, A., Wilke, M., de Wit, M. C. Y., Mancini, G. M. S., Sztriha, L., Im, K., Amrom, D., Andermann, E., Paetau, R., Lehesjoki, A.-E., Walsh, C. A. and Lehtinen, M. K. (2018), 'Sodium Channel SCN3A (NaV1.3) Regulation of Human Cerebral Cortical Folding and Oral Motor Development', *Neuron* **99**(5), 905–913.e7.  
**URL:** <https://www.sciencedirect.com/science/article/pii/S0896627318306500>
- Soofi, W., Archila, S. and Prinz, A. A. (2012), 'Co-variation of ionic conductances supports phase maintenance in stomatogastric neurons', *Journal of Computational Neuroscience* **33**(1), 77–95.  
**URL:** <https://doi.org/10.1007/s10827-011-0375-3>
- Stühmer, W., Ruppersberg, J., Schröter, K., Sakmann, B., Stocker, M., Giese, K., Perschke, A., Baumann, A. and Pongs, O. (1989), 'Molecular basis of functional diversity of voltage-gated potassium channels in mammalian brain.', *The EMBO Journal* **8**(11), 3235–3244.  
**URL:** <https://www.emboress.org/doi/abs/10.1002/j.1460-2075.1989.tb08483.x>
- Taylor, A. L., Goaillard, J.-M. and Marder, E. (2009), 'How Multiple Conductances Determine Electrophysiological Properties in a Multicompartment Model', *Journal of Neuroscience* **29**(17), 5573–5586.
- Tsaur, M.-L., Sheng, M., Lowenstein, D. H., Jan, Y. N. and Jan, L. Y. (1992), 'Differential expression of K<sup>+</sup> channel mRNAs in the rat brain and down-regulation in the hippocampus following seizures', *Neuron* **8**(6), 1055–1067.  
**URL:** <https://www.sciencedirect.com/science/article/pii/089662739290127Y>
- Van Dyke, D. H., Griggs, R. C., Murphy, M. J. and Goldstein, M. N. (1975), 'Hereditary myokymia and periodic ataxia', *Journal of the Neurological Sciences* **25**(1), 109–118.  
**URL:** <https://www.sciencedirect.com/science/article/pii/0022510X75901914>
- Veh, R. W., Lichtinghagen, R., Sewing, S., Wunder, F., Grumbach, I. M. and Pongs, O. (1995), 'Immunohistochemical Localization of Five Members of the KV1 Channel Subunits: Contrasting Subcellular Locations and Neuron-specific Co-localizations in Rat Brain', *European Journal of Neuroscience* **7**(11), 2189–2205.  
**URL:** <https://onlinelibrary.wiley.com/doi/abs/10.1111/j.1460-9568.1995.tb00641.x>
- Verma, P., Kienle, A., Flockerzi, D. and Ramkrishna, D. (2020), 'Computational analysis of a 9D model for a small DRG neuron', *Journal of Computational Neuroscience* **48**(4), 429–444.  
**URL:** <https://doi.org/10.1007/s10827-020-00761-6>
- Wang, F. C., Parcej, D. N. and Dolly, J. O. (1999), 'α Subunit compositions of Kv1.1-containing K<sup>+</sup> channel subtypes fractionated from rat brain using dendrotoxins', *European Journal of Biochemistry* **263**(1), 230–237.  
**URL:** <https://febs.onlinelibrary.wiley.com/doi/abs/10.1046/j.1432-1327.1999.00493.x>

- 617 Wang, H., Kunkel, D. D., Schwartzkroin, P. A. and Tempel, B. L. (1994), 'Localization of Kv1.1  
618 and Kv1.2, two K channel proteins, to synaptic terminals, somata, and dendrites in the mouse  
619 brain', *Journal of Neuroscience* **14**(8), 4588–4599.  
620 **URL:** <https://www.jneurosci.org/content/14/8/4588>
- 621 Waxman, S. G. (2007), 'Channel, neuronal and clinical function in sodium channelopathies: from  
622 genotype to phenotype', *Nature Neuroscience* **10**(4), 405–409.  
623 **URL:** <https://www.nature.com/articles/nn1857>
- 624 Weber, Y. G., Biskup, S., Helbig, K. L., Von Spiczak, S. and Lerche, H. (2017), 'The role of  
625 genetic testing in epilepsy diagnosis and management', *Expert Review of Molecular Diagnostics*  
626 **17**(8), 739–750.  
627 **URL:** <https://doi.org/10.1080/14737159.2017.1335598>
- 628 Xu, J. and Li, M. (1997), 'Kv $\beta$ 2 Inhibits the Kv $\beta$ 1-mediated Inactivation of K<sup>+</sup> Channels in Trans-  
629 fected Mammalian Cells', *Journal of Biological Chemistry* **272**(18), 11728–11735.  
630 **URL:** <https://www.sciencedirect.com/science/article/pii/S0021925818405091>
- 631 Zhang, C.-L., Messing, A. and Chiu, S. Y. (1999), 'Specific Alteration of Spontaneous GABAergic  
632 Inhibition in Cerebellar Purkinje Cells in Mice Lacking the Potassium Channel Kv1.1', *Journal*  
633 *of Neuroscience* **19**(8), 2852–2864.  
634 **URL:** <https://www.jneurosci.org/content/19/8/2852>
- 635 Zhao, J., Petitjean, D., Haddad, G. A., Batulan, Z. and Blunck, R. (2020), 'A Common Kinetic  
636 Property of Mutations Linked to Episodic Ataxia Type 1 Studied in the Shaker Kv Channel',  
637 *International Journal of Molecular Sciences* **21**(20), 7602.  
638 **URL:** <https://www.mdpi.com/1422-0067/21/20/7602>
- 639 Zhou, L., Zhang, C.-L., Messing, A. and Chiu, S. Y. (1998), 'Temperature-Sensitive Neuromuscu-  
640 lar Transmission in Kv1.1 Null Mice: Role of Potassium Channels under the Myelin Sheath in  
641 Young Nerves', *Journal of Neuroscience* **18**(18), 7200–7215.  
642 **URL:** <https://www.jneurosci.org/content/18/18/7200>
- 643 Zuberi, S. M., Eunson, L. H., Spauschus, A., De Silva, R., Tolmie, J., Wood, N. W., McWilliam,  
644 R. C., Stephenson, J. P. B., Kullmann, D. M. and Hanna, M. G. (1999), 'A novel mutation in the  
645 human voltage-gated potassium channel gene (Kv1.1) associates with episodic ataxia type 1 and  
646 sometimes with partial epilepsy', *Brain* **122**(5), 817–825.  
647 **URL:** <https://doi.org/10.1093/brain/122.5.817>

## 648 **Figure/Table/Extended Data Legends**

Figure 1: Characterization of firing with AUC and rheobase. (A) The area under the curve (AUC) of the repetitive firing frequency-current (fI) curve. (B) Changes in firing as characterized by  $\Delta$ AUC and  $\Delta$ rheobase occupy 4 quadrants separated by no changes in AUC and rheobase. Representative schematic fI curves in blue with respect to a reference fI curve (black) depict the general changes associated with each quadrant.

Figure 2: Diversity in Neuronal Model Firing. Spike trains (left), frequency-current (fI) curves (right) for Cb stellate (A), RS inhibitory (B), FS (C), RS pyramidal (D), RS inhibitory +K<sub>V</sub>1.1 (E), Cb stellate +K<sub>V</sub>1.1 (F), FS +K<sub>V</sub>1.1 (G), RS pyramidal +K<sub>V</sub>1.1 (H), STN +K<sub>V</sub>1.1 (I), Cb stellate  $\Delta$ K<sub>V</sub>1.1(J), STN  $\Delta$ K<sub>V</sub>1.1(K), and STN (L) neuron models. Black marker on the fI curves indicate the current step at which the spike train occurs. The green marker indicates the current at which firing begins in response to an ascending current ramp, whereas the red marker indicates the current at which firing ceases in response to a descending current ramp.

Figure 3: The Kendall rank correlation (Kendall  $\tau$ ) coefficients between shifts in  $V_{1/2}$  and AUC, slope factor k and AUC as well as current conductances and AUC for each model are shown on the right in (A), (B) and (C) respectively. The relationships between AUC and  $\Delta V_{1/2}$ , slope (k) and conductance (g) for the Kendall  $\tau$  coefficients highlights by the black box are depicted in the middle panel. The fI curves corresponding to one of the models are shown in the left panels.

Figure 4: The Kendall rank correlation (Kendall  $\tau$ ) coefficients between shifts in  $V_{1/2}$  and rheobase, slope factor k and AUC as well as current conductances and rheobase for each model are shown on the right in (A), (B) and (C) respectively. The relationships between rheobase and  $\Delta V_{1/2}$ , slope (k) and conductance (g) for the Kendall  $\tau$  coefficients highlights by the black box are depicted in the middle panel. The fI curves corresponding to one of the models are shown in the left panels.

Figure 5: Effects of episodic ataxia type 1 associated K<sub>V</sub>1.1 mutations on firing. Effects of K<sub>V</sub>1.1 mutations on AUC ( $AUC_{contrast}$ ) and rheobase ( $\Delta$ rheobase) compared to wild type for RS pyramidal +K<sub>V</sub>1.1 (A), RS inhibitory +K<sub>V</sub>1.1 (B), FS +K<sub>V</sub>1.1 (C), Cb stellate (D), Cb stellate +K<sub>V</sub>1.1 (E), Cb stellate  $\Delta$ K<sub>V</sub>1.1(F), STN (G), STN +K<sub>V</sub>1.1 (H) and STN  $\Delta$ K<sub>V</sub>1.1(I) models V174F, F414C, E283K, and V404I mutations are highlighted in color for each model. Pair-wise Kendall rank correlation coefficients (Kendall  $\tau$ ) between the effects of K<sub>V</sub>1.1 mutations on rheobase and on AUC are shown in J and K respectively.



	RS Pyra- midal	RS Inhib- itory	FS	Cb Stellate	Cb Stellate +K <sub>V</sub> 1.1	Cb Stellate $\Delta$ K <sub>V</sub> 1.1	STN	STN +K <sub>V</sub> 1.1	STN $\Delta$ K <sub>V</sub> 1.1
$g_{Na}$	56	10	58	3.4	3.4	3.4	49	49	49
$g_K$	5.4	1.89	3.51	9.0556	8.15	9.0556	57	56.43	57
$g_{K_V1.1}$	0.6	0.21	0.39	—	0.90556	1.50159	—	0.57	0.5
$g_A$	—	—	—	15.0159	15.0159	—	5	5	—
$g_M$	0.075	0.0098	0.075	—	—	—	—	—	—
$g_L$	—	—	—	—	—	—	5	5	5
$g_T$	—	—	—	0.45045	0.45045	0.45045	5	5	5
$g_{Ca,K}$	—	—	—	—	—	—	1	1	1
$g_{Leak}$	0.0205	0.0205	0.038	0.07407	0.07407	0.07407	0.035	0.035	0.035
$\tau_{max,M}$	608	934	502	—	—	—	—	—	—
$C_m$	118.44	119.99	101.71	177.83	177.83	177.83	118.44	118.44	118.44

Table 1: Cell properties and conductances of regular spiking pyramidal neuron (RS Pyramidal), regular spiking inhibitory neuron (RS Inhibitory), fast spiking neuron (FS), cerebellar stellate cell (Cb Stellate), with additional I<sub>K<sub>V</sub>1.1</sub> (Cb Stellate  $\Delta$ K<sub>V</sub>1.1 ) and with I<sub>K<sub>V</sub>1.1</sub> replacement of I<sub>A</sub> (Cb Stellate  $\Delta$ K<sub>V</sub>1.1 ), and subthalamic nucleus neuron (STN), with additional I<sub>K<sub>V</sub>1.1</sub> (STN  $\Delta$ K<sub>V</sub>1.1 ) and with I<sub>K<sub>V</sub>1.1</sub> replacement of I<sub>A</sub> (STN K<sub>V</sub>1.1 ) models. All conductances are given in mS/cm<sup>2</sup>. Capacitances ( $C_m$ ) and  $\tau_{max,M}$  are given in pF and ms respectively.

655 **Extended Data**

656 Extended Data 1: TODO: Caption for code in zip file.

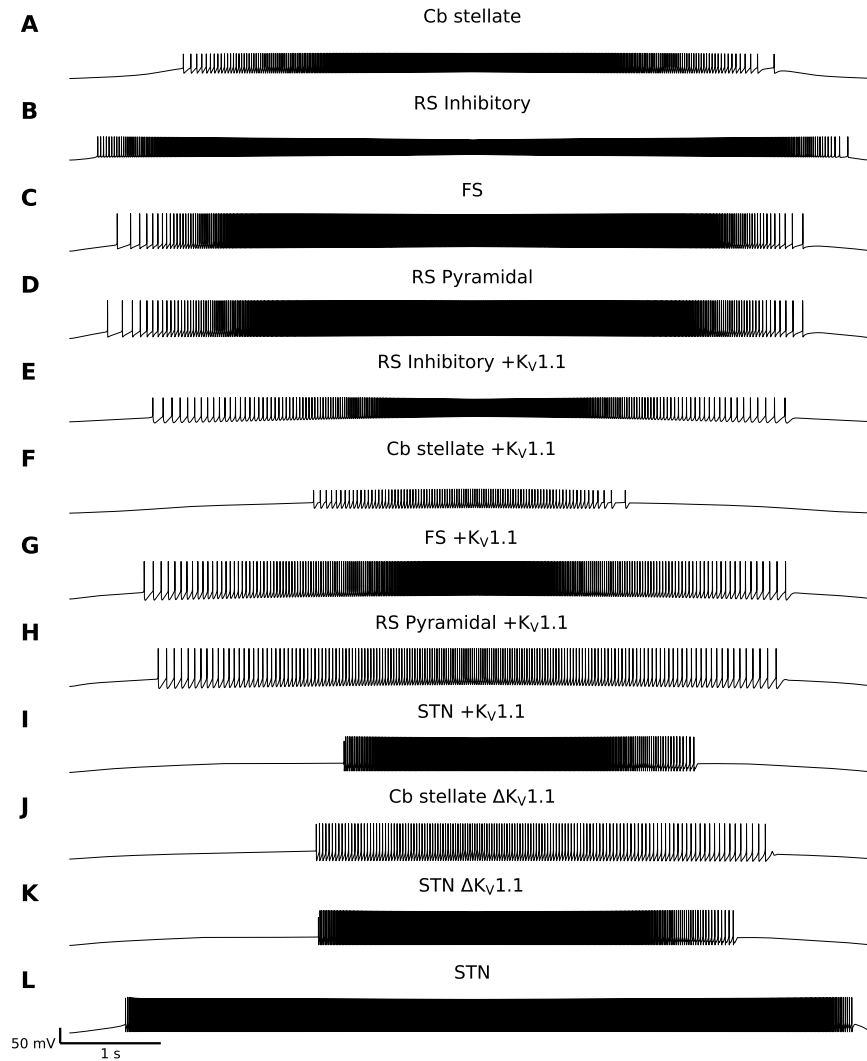


Figure 2-1: Diversity in Neuronal Model Firing Responses to a Current Ramp. Spike trains for Cb stellate (A), RS inhibitory (B), FS (C), RS pyramidal (D), RS inhibitory +K<sub>V</sub>1.1 (E), Cb stellate +K<sub>V</sub>1.1 (F), FS +K<sub>V</sub>1.1 (G), RS pyramidal +K<sub>V</sub>1.1 (H), STN +K<sub>V</sub>1.1 (I), Cb stellate  $\Delta$ K<sub>V</sub>1.1 (J), STN  $\Delta$ K<sub>V</sub>1.1 (K), and STN (L) neuron models in response to a slow ascending current ramp followed by the descending version of the current ramp. The current at which firing begins in response to an ascending current ramp and the current at which firing ceases in response to a descending current ramp are depicted on the frequency current (f) curves in Figure 2 for each model.